The Petrology and Geochemistry of Quartzofeldspathic Gneisses, Broken Hill Mines Area, Broken Hill, New South Wales

BRYAN E. CHENHALL and EVAN R. PHILLIPS

CHENHALL, B. E., & PHILLIPS, E. R. The petrology and geochemistry of quartzofeldspathic gneisses, Broken Hill mines area, Broken Hill, New South Wales. *Proc. Linn. Soc. N.S.W.* 108 (1), (1984) 1985: 1-21.

Two composite, elongate bodies consisting predominantly of quartzofeldspathic gneiss and quartzofeldspathic rocks, together with subordinate volumes of interlayered 'amphibolite/basic granulite' and pegmatite crop out on both the western and eastern sides of the Broken Hill orebody. The compositional diversity present in both bodies is consistent with their origin as a composite pile of volcanic and sedimentary rocks. Initial granulite facies metamorphism of the bodies was overprinted by a greenschist to amphibolite facies retrograde event localized in and adjacent to retrograde schist zones. Three major types of quartzofeldspathic gneiss are defined and described. Granulite facies assemblages and microstructures are largely preserved throughout these gneissic types. Nevertheless, most representative samples are 'polymetamorphic' for they display intergranular/intragranular microstructures and compositional readjustments between biotite and garnet consistent with lower ($<600°C$) metamorphic temperatures. Microstructures in which various morphological types of microperthite are spatially associated with myrmekite appear to have evolved by an exsolution mechanism. Compositional shifts of garnet and biotite towards more Mg-rich endmember compositions with prograde metamorphism, are overprinted by retrograde reactions involving shift in garnet and biotite compositions towards more Fe- and Mg-rich species respectively. Retrograde garnet and biotite compositions are preserved in garnet rims and in domains adjacent to garnet-biotite interfaces. The metastable persistence of orthoclase throughout quartzofeldspathic gneisses is attributed to a 'dry' cooling history where water activity (a_{H_2O}) <1.

B. E. Chenhall and E. R. Phillips (deceased), Department of Geology, University of Wollongong, Post Office Box 1144, Wollongong, Australia 2500; *manuscript received 1 May 1984, accepted for publication 25 July 1984.*

INTRODUCTION

Quartzofeldspathic gneiss is the name given to distinctive light cream to mid-grey, foliated rocks containing quartz, feldspar (sodic plagioclase and/or K-feldspar) and biotite as essential minerals, with almandine and sillimanite as additional phases in some samples. Such rocks are abundant and widespread throughout the Broken Hill Block of the Willyama Complex (Stillwell, 1922; Binns, 1962, 1964) being exposed in western New South Wales and eastern South Australia (Fig. 1**A**).

Within the Broken Hill mines area, surface exposures and numerous diamond drill intersections delineate two major bodies of quartzofeldspathic gneiss cropping out as elongate bodies for about 30km along each side of the main Broken Hill orebody (Fig. 1**B**). Carruthers and Pratten (1961) named these rocks the upper granite gneiss (west) and the lower granite gneiss (east) and suggested that they represent the upper and lower units in a stratigraphic succession termed the mine sequence. However, recent detailed work by Laing *et al.* (1978) indicates that the two quartzofeldspathic gneiss bodies are probably stratigraphic equivalents in a tightly-folded sequence. Throughout this paper we have simply used the names western quartzofeldspathic and eastern quartzofeldspathic gneiss when referring to the two bodies.

Previous work indicated that the western and eastern quartzofeldspathic gneisses are somewhat different in field appearance but that there are no consistent mineralogical or chemical criteria to distinguish between them (Johnson and Klingner, 1975). On

petrological and geochemical grounds, three major types of quartzofeldspathic gneiss are defined in this study. Two of these types are present in the eastern body. The aims of this work are to describe and compare the petrographic, mineralogical and geochemical characteristics of these gneisses and to discuss the nature of their parent material prior to regional metamorphism.

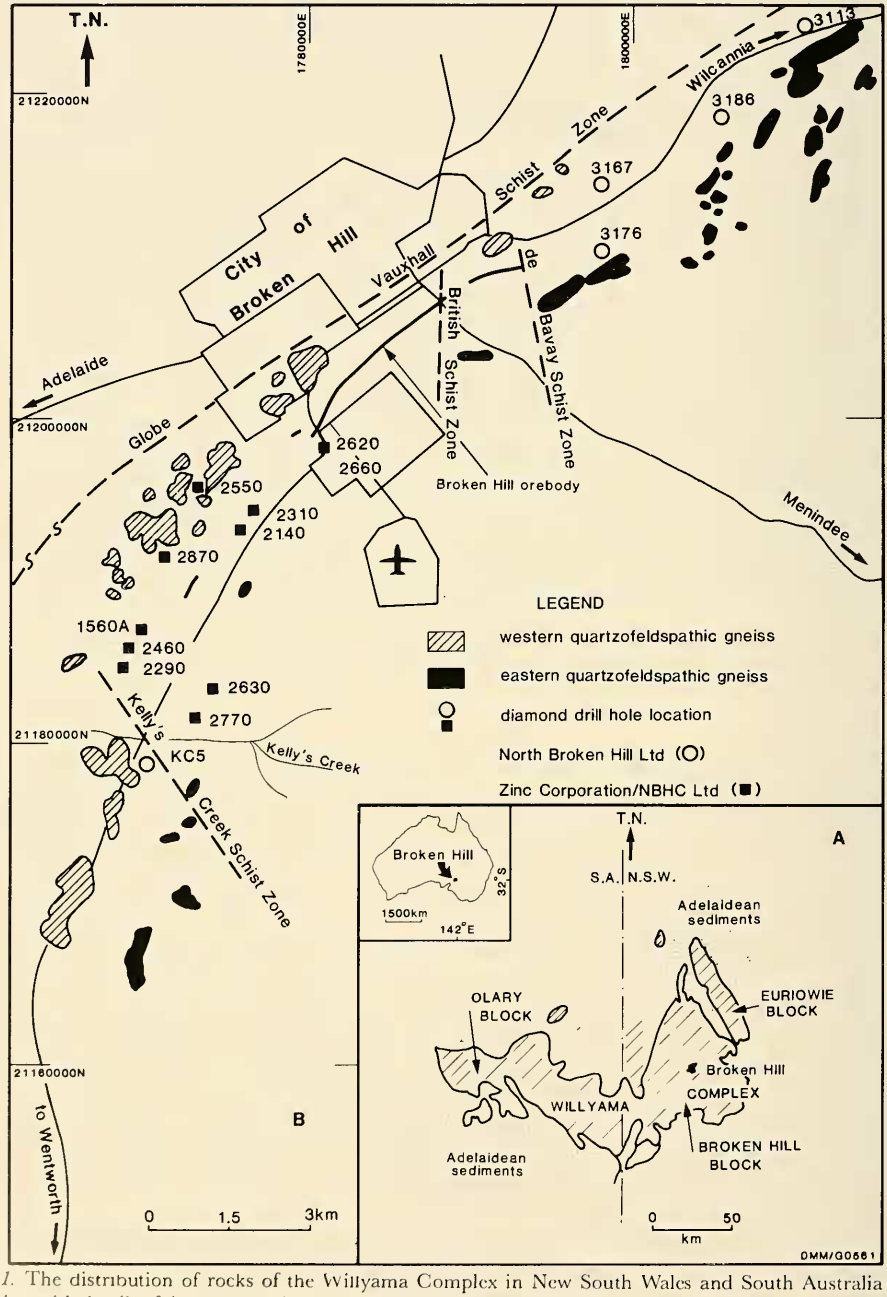

Fig. 1. The distribution of rocks of the Willyama Complex in New South Wales and South Australia (**A**) together with details of the outcrop distribution (**B**) of the western and eastern quartzofeldspathic gneiss in the Broken Hill mines area (adapted from the AIMM geological map of Broken Hill, 1968).

Structural and Metamorphic Setting of the Western and Eastern Quartzofeldspathic Gneisses

Since the early part of the twentieth century there have been numerous attempts to interpret the structure of the Broken Hill orebody and enclosing rocks (e.g. Andrews, 1922; King and O'Driscoll, 1953; Carruthers and Pratten, 1961; Hobbs, 1966). Quite recently, however, Laing *et al.* (1978) and Laing (1980) have published a detailed reinterpretation of the macroscopic structure in the Broken Hill mines area. These workers suggest that the orebody lies in an antiformal structure (Broken Hill Antiform) between two synforms, the Hanging Wall Synform and Broken Hill Synform, which respectively contain the western and eastern quartzofeldspathic gneisses (Laing, 1980: fig. 4.5). These folds represent macroscopic F2 structures superimposed on a 'stratigraphic succession' which had previously been inverted (Laing, 1980). The western and eastern quartzofeldspathic gneisses are thus regarded as being equivalent stratigraphic units and, because of the inverted attitude of the succession, represent metamorphic Suite 3, the oldest rocks exposed in the Broken Hill mines area. The Broken Hill antiform contains stratigraphically younger rocks of the 'mine sequence' (Suite 4) including sillimanite schist and gneiss, psammitic schist, Potosi gneiss and amphibolite/hornblende-pyroxene granulite together with bodies of Pb-Zn sulphides and lode horizon rocks (see Johnson and Klingner, 1975).

Metamorphic studies by Binns (1962, 1964) show that rocks of the Willyama Complex have undergone initial prograde regional metamorphism under conditions ranging from the amphibolite to granulite facies. Metamorphic grade, in general, increases from northwest to southeast across the orebody (Binns, 1964; Chenhall, 1976; Plimer, 1976; Phillips, 1980). Phillips (1980) has estimated peak metamorphic temperatures in the vicinity of the Broken Hill mines area to have been $< 810°C$ with water activity (a_{H_2O}) estimates (from metapelite data) in the range 0.5 - 0.6. Scott, Both and Kissin (1976) suggested a pressure range of 7.8 - 8.3 kb based on coexisting sphalerite-pyrrhotite pairs from the main orebody although Phillips (1980) has concluded that a more realistic estimate of the upper pressure limit of regional metamorphism in the Broken Hill Block is around 6 kb. This prograde metamorphic event has been dated at 1640 ± 40 m.y. and 1695 ± 21 m.y. by Pidgeon (1967) and Shaw (1968) respectively.

Later retrograde metamorphism along essentially planar zones, termed retrograde schist zones (Vernon, 1969; Vernon and Ransom, 1971) has locally converted the original coarse schistose or gneissic fabric to a finer one in which the mineral assemblages are characteristic of the amphibolite facies (Vernon, 1969; Chenhall, 1973). Additionally, less intense, widespread pseudomorphous retrogression has more or less modified the prograde rocks outside these zones (Vernon, 1969; Chenhall, 1973).

Western Quartzofeldspathic Gneiss

The western quartzofeldspathic gneiss is a composite mass consisting largely of quartzofeldspathic gneisses with subordinate amounts of 'amphibolite/basic granulite', metapelite and relatively abundant bodies of pegmatite which are generally concordant with the gneissic foliation. Quartzofeldspathic gneiss / 'amphibolite / basic granulite' contacts are generally sharp and no discernible mineralogical gradation is evident between the two rock types. Samples of 'amphibolite/basic granulite' collected at the contacts with quartzofeldspathic gneisses commonly display a schistose fabric and appear to have retrogressed to assemblages dominated by biotite or by biotite, hornblende, quartz and plagioclase.

Retrogression is by no means confined to the basic gneisses at these contacts. Detailed petrographic studies show that many samples of quartzofeldspathic gneiss have been mildly to moderately affected by retrograde metamorphism. Microstructures

indicative of retrograde readjustments include recrystallization of coarse prograde quartz, feldspar and biotite, the replacement of almandine by biotite and of K-feldspar by aggregates of sericite and muscovite. Only those gneisses with a coarse prograde microstructure and showing little or no development of minerals of retrograde origin are described in detail below.

The quartzofeldspathic gneisses of the western mass range from mid grey, moderately well-foliated biotite gneiss to pale grey to cream quartz- and/or feldspar-rich varieties including finer grained aplitic phases together with rare barium feldspar-bearing variants (Mawson and Segnit, 1946). In the quartz-feldspar rich rocks and in some very coarse gneisses, the fabric is represented by a crude biotite lineation rather than a foliation.

The most common type of mid-grey biotite gneiss is medium (1mm) to coarse (2cm) grained and is characterized by a wavy and rather irregular gneissic foliation defined by discontinuous biotite clusters. Gneisses possessing these characteristics are present in most surface outcrops to the south of Broken Hill and are especially well represented in cores from DDH 2550 and DDH 2870 drilled to the south of the city (Fig. 1**B**). Most samples are relatively even grained but locally they are observed to contain numerous megacrysts of K-feldspar. Where developed, ovoid K-feldspar megacrysts (< 1cm in size) and xenoblastic almandine porphyroblasts show a preferred dimensional orientation parallel to the foliation.

TABLE 1

Modal ranges for the western and eastern quartzofeldspathic gneisses

	Western Gneiss				Eastern Gneiss							
					Type 1				Type 2			
	> 5% K-feld		< 5% K-feld		> 5% K-feld		< 5% K-feld		> 5% K-feld		< 5% K-feld	
	range		range		range		range		range		range	
%	min.	max.	min.	max.	min.	max.	min.	max.	min.	max	min.	max.
Quartz	30	49	34	53	30	50	33	49	34	46	30	50
Plagioclase	14	31	15	48	1	34	25	44	17	28	17	44
Microperthite	7	42	0	4	13	48	0	5	15	16	2	5
Biotite	3	35	3	20	4	17	7	29	7	16	7	19
Garnet	0	19	0	20	0	3	0	8	0	10	0	22
Opaques/Muscovite	1.1	9	6	6	0	6	1	6	1	6	0	2.4
Sillimanite	0	4.4	0	2								
Number of Samples	28		20		23		10		2		10	

Source: Stone, 1973: Pemberton, 1977.

Two mineralogically distinct subtypes of the typical mid grey gneiss have been recognized in thin section. One subtype is free from or low in K-feldspar (< 5% by mode) and the other contains significant amounts of this mineral. Modal ranges for these rocks are presented in Table 1. The field relationships between these two subtypes are difficult to discern since the rocks have similar physical appearance in handspecimen. However, modal data obtained from cores sampled at intervals of 30cm or less appear to indicate that the two subtypes can exhibit an interlayered relationship. Furthermore, both subtypes appear to be represented in most outcrops and diamond drill cores. Thin sections of

both variants are seen to consist of xenoblasts of quartz, clear unzoned twinned plagioclase (composition An_{30}-An_{42}) and subidioblastic, strongly pleochroic (α = pale straw, $\beta = \gamma$ = dark chestnut or red-brown) biotite. Quartz and plagioclase grains are approximately equal in size (1-2mm) and form granoblastic aggregates. Some plagioclase crystals show the development of antiperthitic intergrowths. Biotite flakes (0.5-2mm in size) tend to be grouped together forming discontinuous, flattened folia up to 1cm in length. In most samples the biotite flakes are rimmed with distinctive, thin coronas of very fine (<0.1mm) ilmenite granules. Fine (0.1mm) needles of ilmenite are concentrated in the biotite {001} cleavages.

K-feldspar, where present in modal amounts exceeding 5%, occurs as untwinned xenoblasts, commonly coarser (up to 2cm) than the adjacent quartz and plagioclase grains. X-ray diffraction studies indicate that the K-feldspar is orthoclase. Most K-feldspar crystals are microperthitic, the dominant morphological forms being patch and film microperthite. Rim myrmekite is sporadically developed along the margins of the orthoclase crystals in many rocks and intergranular myrmekite is common. Approximately sixty percent of both the K-feldspar-free and K-feldspar-bearing gneiss contain sillimanite as wavy irregular trains of prisms, as patches of fine stumpy prisms or as fibrolite mats, all of which are intergrown with biotite folia. Almandine is present in most rocks and occurs either as coarse (up to 1cm) elongate, cracked xenoblasts containing lobate inclusions of quartz and biotite and needles of sillimanite, or as smaller (1-2mm) grains partly rimmed by biotite. Fine (0.1-0.5mm) needles of sillimanite are common as inclusions in almandine and these define an internal lineation subparallel to that defined by the coarser sillimanite rods associated with the biotite folia. Fine grained (0.05-0.2mm) biotite (which is optically indistinguishable from that forming the folia) is commonly dispersed along the cracks in the almandine xenoblasts along with minor amounts of fine grained (0.05-0.1mm) green biotite (electron probe identification) and sericitic muscovite.

Eastern Quartzofeldspathic Gneiss

Detailed field observation and logging of diamond drill cores together indicate that the eastern quartzofeldspathic gneiss is also a composite body consisting mostly of quartzofeldspathic gneiss with subordinate volumes of 'amphibolite/basic granulite', metapelite and pegmatite. Layers of 'amphibolite/basic granulite' (from 30cm to 30m in thickness) are more abundant within and are almost continuously developed along both western and eastern margins of the quartzofeldspathic rocks composing this body. Quartzofeldspathic gneisses in the eastern mass display considerable lithological diversity, ranging from quartz- and/or feldspar-rich, generally poorly-foliated types, including finer aplitic phases and rare anorthositic variants (Chenhall *et al.*, 1977), through to well-foliated varieties containing more than 10% modal biotite. Retrograde features similar to those given in relation to the western quartzofeldspathic gneiss are widespread and are not considered below.

Two major types of quartzofeldspathic gneiss are present. The first type is represented in the bold outcrops to the northeast of the de Bavay Schist Zone and also in scattered outcrops to the south of Broken Hill near the Kelly's Creek Schist Zone. This gneissic type cannot be traced continuously along strike owing to poor exposure to the south of Broken Hill (Fig. 1**B**). Type 1 gneisses occur in diamond drill holes 2620, 2660, 2310 and 2140. The second type is restricted in occurrence to isolated outcrops southwest of the de Bavay Schist Zone. This gneiss has not been observed in the Kelly's Creek area but it is well represented in diamond drill holes 1560A, 2630 and 2770. Gneisses having type 2 characteristics are also present in DDH 2620, 2660, 2310 and 2140.

The structural relationship between the two types of gneiss is uncertain for they have not been observed together in outcrop. Information from diamond drill cores tends to indicate that, with respect to the type 1 gneisses, the type 2 gneisses occupy a structurally higher (that is stratigraphically lower) position in the Broken Hill Antiform.

Type 1

Samples of the gneiss range from cream (surface exposures) to mid-grey (subsurface) and commonly display a well-developed almost platy foliation defined by nearly continuous biotite folia. Both K-feldspar-free and K-feldspar-bearing rocks are well represented in this type (Table 1) and are irregularly distributed throughout single outcrops and individual diamond drill hole cores. In thin sections the rocks are seen to consist of granoblastic aggregates of medium grained (0.5-1.5mm) xenoblasts of quartz and essentially unzoned twinned plagioclase having a composition range $An_{15}-An_{28}$. Pleochroic (α = pale straw, $\beta = \gamma$ = deep red-brown or chestnut) subidioblastic biotite flakes (containing fine, ilmenite needles) averaging 0.5-1mm in size define the foliation in these rocks. Where present, most K-feldspar grains occur as xenoblasts similar in size to those of quartz and plagioclase. The K-feldspar crystals are either untwinned or display twinning ranging from a shadowy, crosshatching through to a well-defined tartan pattern. X-ray diffraction studies indicate that most of the K-feldspar is orthoclase, although there is some broadening (but no discernible splitting) of the 131 peak in grains displaying shadowy twinning. Grains with tartan twinning are intermediate microcline. Two morphological types of microperthite occur in the K-feldspar grains. In one type the sodic plagioclase forms 'beads' associated with fine film perthite and the rocks contain rim and intergranular albite but no myrmekite. In the other type, regular film perthites are observed in close spatial arrangement with rim and intergranular myrmekite (An_{15}-An_{17}) and distinctive, thin albite rims are developed along the margins of adjacent plagioclase crystals.

Almandine is an uncommon mineral in gneisses northeast of the de Bavay Schist Zone but locally becomes more abundant in rocks southwest of this zone. Where present, the almandine either occurs as equidimensional cracked xenoblastic (up to 1cm in size) porphyroblasts or as finer (0.2-2mm) xenoblastic grains. Garnet grains are commonly mantled by and their cracks infilled with fine grained (0.1mm) biotite of similar pleochroic scheme to that forming the folia in the gneisses. Minor green biotite and very pale green 'phengite' also occur in cracks in the garnet.

Type 2

Specimens of this mid-grey type are characterized by a moderately developed irregular and wavy foliation defined by discontinuous aggregates of biotite. Modal ranges for this gneiss are given in Table 1. In thin section, xenoblastic quartz, plagioclase and in some samples untwinned K-feldspar (orthoclase) commonly range from 0.2mm up to 1.5mm in size. Rarely, xenoblasts of quartz and plagioclase may reach 3mm in length. Plagioclase occurs as unzoned, twinned crystals, albite and pericline twins predominating over Carlsbad twins. Compositions of plagioclases range from An_{34} to An_{60} with typical compositions in the range An_{40} to An_{45}. Pleochroic (α = pale straw, $\beta = \gamma$ = deep red brown or dark brown) subidioblastic to xenoblastic biotite, ranging from 0.2mm up to 1mm in length, occurs as discontinuous clusters (up to 3mm in length) sparsely dispersed throughout the quartz-feldspar matrix. Needles and granules of ilmenite occur as inclusions in most biotite grains and coronas of fine (<0.05mm) ilmenite granules are sporadically developed along their margins. Almandine is a common mineral in this type of the eastern gneiss. Garnet usually forms as sub-spherical to irregular, lobate, xenoblastic porphyroblasts ranging from 3mm up to 1cm in size. Crystals of almandine are sparsely

poikiloblastic, common inclusions being biotite and quartz. Rare, very fine (<0.05mm) needles of sillimanite are present in almandines from some samples of this type. Fractures in the garnet xenoblasts commonly contain fine brown biotite and minor green biotite and sericitic muscovite.

Chemical Data

Sample Selection Procedure

Two criteria have been adopted for sample selection in this study. First, as indicated above, the chosen samples have their prograde mineralogy and microstructure largely preserved and are free from, or have low (<6%) modal percentages of, minerals of retrograde character such as muscovite. It is to be noted that many samples of both gneisses fail to meet the requirements of this criterion and have been rejected. Second, only those rocks which are typical of a particular field exposure or diamond drill core log have been analysed.

One disadvantage of this second criterion is that it makes no allowance for some of the compositional diversity present in both gneissic masses. Nevertheless this method of selection has been used since it offers a means of chemical comparison between samples from both the eastern and western quartzofeldspathic gneiss.

Whole Rock Data

Tables 2 and 3 list major and trace element data for typical samples of the western and eastern quartzofeldspathic gneisses respectively. Sample localities are presented in an Appendix. Mean oxide and trace element compositions, together with standard deviations have been calculated and are presented for the data of Tables 2 and 3. Three analyses of quartz- and feldspar-rich rocks constituting minor layers in the eastern quartzofeldspathic gneiss are also given in Table 3. These are included to illustrate some of the compositional diversity generally to be expected throughout quartzofeldspathic gneisses in the Broken Hill mines area.

Tables 2 and 3 also give an indication of the within-type compositional ranges present in the three main gneissic groups defined in this study. These tables show that there are considerable differences in composition between type 1 of the eastern gneiss (where SiO_2 is generally >70%, Al_2O_3<15%, calculated total iron as FeO <5% and TiO_2 <0.5% by weight) and the other two gneisses (where SiO_2 is generally <70%, Al_2O_3 >15%, FeO >5% and TiO_2 >0.5% by weight) which are seen to be chemically similar. Figs 2**a**, 2**b** and 2**c** show that Al_2O_3, total iron as FeO and TiO_2 contents are linearly related to SiO_2 composition, type 1 gneisses being distinguished from the other rocks on the basis of lower Al_2O_3/SiO_2, FeO/SiO_2 and TiO_2/SiO_2. Moreover, these plots show small scatter about the pooled sample (n = 37) regression lines and indicate that respectively 69%, 79% and 85% of the variation (calculated as $100r^2$ where r is the correlation coefficient) in Al_2O_3, FeO and TiO_2 is explained by the variation in SiO_2. A pooled sample is used since the regression coefficients obtained by least squares fitting of individual groups have similar magnitudes. Chemical plots of FeO/Al_2O_3, (Fig. 2**d**) and Na_2O/CaO (Fig. 3**a**) show considerable scatter; the degree of scattering and small within-group sample size tending to obscure systematic relationships (based on a regression model) between these oxides. However, type 1 rocks generally have lower FeO/Al_2O_3 compared with the other gneisses. Fig. 3**a** indicates that type 2 gneisses have higher CaO/Na_2O compared with samples of the western quartzofeldspathic gneiss and this chemical attribute is reflected in the compositional range of their plagioclases, An_{30}-An_{42} and An_{34}-An_{60} respectively.

All gneissic groups show considerable variation with respect to their K_2O, Na_2O and

TABLE 2

Chemical data for the western quartzofeldspathic gneiss

K – feldspar bearing gneisses

Specimen Number	2908	2926	2913	4150	2916	4154	4162
SiO_2	75.25	67.91	67.52	67.33	67.18	71.61	65.96
TiO_2	.15	.62	.60	.69	.69	.24	.73
Al_2O_3	13.26	15.36	15.41	14.88	15.41	16.25	16.83
Fe_2O_3	.02	.53	.78	.08	.25	.17	1.23
FeO	1.28	4.27	4.53	6.07	4.61	1.83	4.61
MnO	.02	.06	.07	.10	.04	.02	.10
MgO	.24	.92	1.08	1.08	1.05	.40	1.47
CaO	.51	1.55	1.60	1.77	1.91	.84	1.11
Na_2O	2.34	2.91	2.33	2.42	2.89	2.80	.79
K_2O	5.30	4.18	4.46	3.93	4.54	5.72	4.76
P_2O_5	.11	.11	.12	.15	.12	.14	.70
L.O.I.	1.90	1.39	1.07	.88	1.05	.79	2.00
FeO (total)	1.30	4.75	5.23	6.14	4.83	1.98	5.72
Mol. Al_2O_3/(K_2O + CaO + Na_2O)	1.26	1.27	1.33	1.30	1.17	1.32	1.93
TOTAL	99.57	99.81	99.57	99.38	99.74	100.81	99.89
Y	26	85	63	68	80	50	68
Sr	89	178	113	117	78	89	115
Zr	67	385	238	268	273	124	284
Nb	11	28	19	25	24	18	–
Rb	307	159	212	221	248	275	233
Th	9	39	22	24	24	16	25
Pb	68	60	27	29	26	26	43

K – feldspar deficient gneisses

	4409	2903	2835	4171	4151	4152	4153	2902	2897	2858	$\bar{X}$	S
SiO_2	65.25	69.23	66.12	68.27	68.01	70.21	69.33	67.00	67.57	66.11	68.23	2.43
TiO_2	.87	.54	.16	.63	.69	.64	.62	.67	.65	.62	.61	.17
Al_2O_3	15.53	14.95	16.39	15.51	15.79	14.48	15.72	15.63	16.00	16.18	15.48	.78
Fe_2O_3	.75	.17	.58	.24	.34	.31	.25	.64	.34	.42	.42	.31
FeO	6.49	4.52	4.92	3.35	3.63	6.32	2.49	3.89	4.88	5.61	4.31	1.47
MnO	.12	.08	.03	.02	.03	.05	.03	.03	.06	.12	.06	.04
MgO	1.38	.87	1.02	.92	.95	1.03	.96	1.08	1.29	1.20	1.00	.31
CaO	3.67	3.00	1.22	2.35	3.13	2.66	3.34	3.23	3.07	2.02	2.18	.97
Na_2O	2.88	3.66	1.74	3.08	3.55	3.11	4.42	4.31	3.18	3.28	2.94	.86
K_2O	1.58	1.33	4.76	4.47	2.54	1.60	1.37	1.93	1.50	2.77	3.34	1.56
P_2O_5	.13	.13	.12	.15	.11	.15	.16	.17	.14	.11	.17	.14
L.O.I.	.27	1.27	1.90	.23	.36	.72	.67	1.07	1.30	1.53	1.08	.55
FeO (total)	7.16	4.67	5.44	3.57	3.94	6.60	2.71	4.47	5.19	5.99		
Mol. Al_2O_3/(K_2O + CaO + Na_2O)	1.18	1.16	1.55	1.09	1.11	1.24	1.06	1.04	1.29	1.34		
TOTAL	98.12	99.75	99.66	99.22	99.14	99.28	99.36	99.65	99.98	99.97		
Y	90	86	89	49	53	56	64	60	64	69	66	17
Sr	308	416	145	268	152	273	566	351	454	143	227	147
Zr	229	351	400	244	270	237	245	266	273	253	259	80
Nb	26	30	31	22	41	25	30	23	23	20	25	7
Rb	90	65	215	201	155	96	89	66	90	156	169	77
Th	–	31	43	49	–	22	30	24	23	23	27	10
Pb	–	39	30	32	–	25	30	18	20	61	36	16

Analysts. S.E. Shaw, R.H. Flood and B.E. Chenhall.

Locality information given in Appendix 1.

TABLE 3

Chemical data for the eastern quartzofeldspathic gneiss

TYPE 1 GNEISSES

	K – feldspar bearing gneisses								K – feldspar deficient gneisses				
Sample	4119	2931	2851	2928	4120	4205	4194	4196	4392	4396	2932	$\bar{x}$	s
SiO_2	73.08	73.94	72.50	73.41	73.40	73.59	71.22	72.79	70.99	70.04	71.36	72.01	1.45
TiO_2	.39	14	31	.15	26	23	48	.45	.50	57	48	.42	.14
Al_2O_3	13.45	13.41	13.44	13.60	13.44	14.08	12.91	13.09	14.97	14.28	14.23	13.80	.79
Fe_2O_3	71	02	05	04	21	42	63	.54	88	90	50	.60	.27
FeO	2.56	1.57	2.80	1.75	1.94	1.58	3.54	2.16	2.80	3.45	2.67	2.58	.81
MnO	04	01	02	01	04	03	06	02	.12	05	04	05	.04
MgO	60	34	44	36	56	46	84	61	89	92	83	71	19
CaO	1.07	70	1.43	61	92	67	1.49	1.42	2.90	2.30	2.74	1.62	84
Na_2O	2.06	3.23	3.21	3.68	2.30	3.23	2.39	2.85	1.50	1.06	4.01	2.22	81
K_2O	4.86	5.20	4.56	5.42	5.56	4.52	4.34	4.58	1.99	3.94	1.96	4.16	1.19
P_2O_5	15	20	16	20	.18	15	.15	.08	.10	.11	.16	.13	.04
L.O.I	.50	92	97	68	1.27	1.09	1.13	.64	2.06	1.98	96		
FeO (total)	3.35	1.59	2.86	1.79	2.17	2.05	4.24	2.76	3.78	4.45	3.23		
Mol. Al_2O_3/(K_2O + CaO + Na_2O)	1.27	1.19	1.05	1.04	1.17	1.23	1.14	1.07	1.51	1.40	1.04		
TOTAL	99.47	99.78	99.89	99.85	100.08	100.05	99.18	99.23	99.79	99.70	99.94		
Y	58	46	51	48	43	41	90	71	49	69	57	56	15
Sr	175	84	103	55	114	63	117	73	327	151	260	138	86
Zr	181	68	142	81	118	82	202	172	172	195	187	145	50
Nb	18	11	24	13	23	17	17	14	–	–	18	17	4
Rb	314	430	337	525	359	442	149	275	115	143	134	293	142
Th	17	13	15	11	15	11	14	15	23	27	22	17	5
Pb	13	15	18	13	17	19	21	15	10	13	11	15	3

TYPE 2 GNEISSES

	K – feld bearing gneisses	K – feldspar deficient gneisses										Quartz and feldspar rich minor rock types		
	2862	4124	4189	4138	4384	4386	4139	4128	4129	$\bar{x}$	s	4142	4127	4199
SiO_2	68.89	65.57	65.27	66.26	68.30	68.47	66.72	63.46	65.47	66.49	1.79	83.15	81.20	73.57
TiO_2	.47	.62	.75	.72	58	67	.66	.86	.82	.68	.12	28	.44	.72
Al_2O_3	14.48	16.79	15.64	15.34	15.04	16.32	16.30	16.08	16.52	15.83	.76	8.77	9.93	12.05
Fe_2O_3	.26	.21	.62	.53	.85	1.24	.91	.88	.74	.69	.33	.54	.04	.24
FeO	4.63	5.85	6.19	6.66	4.40	3.40	4.50	6.56	5.16	5.26	1.12	2.08	2.20	2.77
MnO	.05	.15	.25	.09	.08	.09	.10	.14	.10	.12	.06	.09	.02	.05
MgO	.98	1.22	1.14	1.31	1.08	1.14	1.15	1.47	1.47	1.22	.17	.62	.85	1.10
CaO	2.40	3.18	4.09	2.41	2.63	1.92	2.72	2.87	4.08	2.92	.74	2.35	3.10	.73
Na_2O	2.78	2.59	1.95	2.71	1.24	1.65	.96	1.14	3.16	2.02	.82	.38	1.30	.10
K_2O	3.84	2.71	1.95	3.04	3.00	2.79	3.07	3.29	1.65	2.82	.67	.36	.84	6.78
P_2O_5	.12	.08	.16	.14	.09	.10	.11	.10	.05	.11	.03	.01	.04	.01
L.O.I.	1.08	1.62	1.29	.81	2.32	1.81	2.40	2.66	1.14			.72	.62	1.76
FeO (total)	4.92	6.08	6.88	7.25	5.34	4.78	5.51	7.54	5.98			2.68	2.24	3.04
Mol. Al_2O_3/(K_2O + CaO + Na_2O)	1.11	1.29	1.23	1.26	1.49	1.77	1.66	1.51	1.15			1.66	1.14	1.35
TOTAL	99.98	100.59	99.30	100.02	99.77	99.77	99.77	99.72	100.36			99.41	100.58	100.05
Y	137	68	103	69	38	64	45	79	73	75	30	19		6
Sr	188	206	253	105	153	164	137	146	218	174	46	225		183
Zr	155	208	214	211	182	271	172	230	271	213	40	195		13
Nb	11	10	19	20	–	–	–	–	20	16	5	–		–
Rb	191	115	119	175	159	139	138	149	121	145	26	13		261
Th	20	19	22	19	23	27	25	30	36	25	6	10		20
Pb	33	27	80	22	31	23	25	30	21	32	18	15		31

Analysts: S.E. Shaw, R.H. Flood and B.E. Chenhall

Major element analyses for rocks 4119, 2931, 2851, 2928 and 2932 are given in Chenhall et al. (1977). Data not available for 4123

Locality information given in Appendix 1

CaO contents and consequently dispersions (indicated by the magnitude of the standard deviation) about their respective oxide means are relatively large. Fig. 3**b** shows that Na_2O plus CaO contents are linearly related to K_2O composition, although there is considerable scatter (with r = -0.64) about the pooled sample regression line. Compositional contrasts in $K_2O/(Na_2O + CaO)$ are most clearly indicated in Fig. 3**b** for samples of the western quartzofeldspathic gneiss, but a similar range of composition is evident among samples of the other gneisses. These compositional differences are reflected in an inverse relationship between modal K-feldspar and plagioclase contents (Table 1). Most gneisses have molar proportions of $Al_2O_3/(K_2O + Na_2O + CaO)$ in excess of 1.1. As far as can be ascertained, there is no relationship between the magnitude of this molar ratio and the abundance of modal sillimanite in the gneisses.

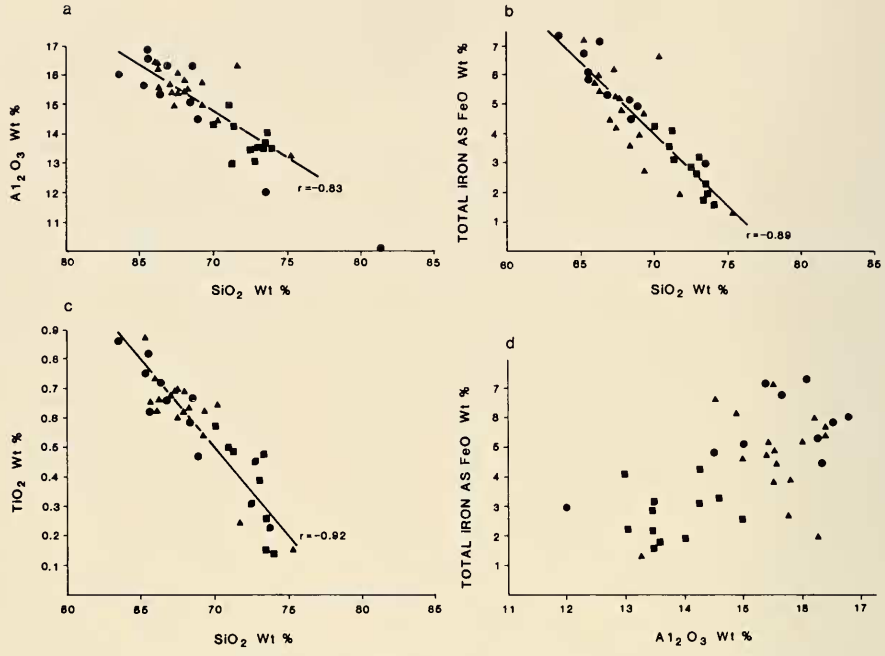

Fig. 2. Chemical plots of Al_2O_3 vs SiO_2 (**a**), FeO vs SiO_2 (**b**), TiO_2 vs SiO_2 (**c**), and FeO vs Al_2O_3 (**d**) for typical western quartzofeldspathic gneiss (▲) and types 1 (■) and 2 (•) of the eastern quartzofeldspathic gneiss.

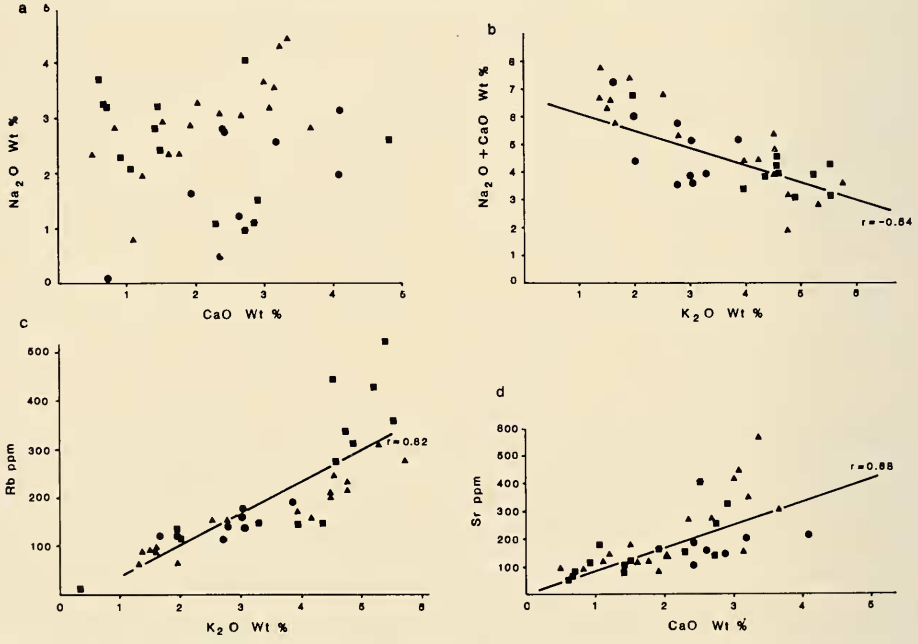

Fig. 3. Chemical plots of Na_2O vs CaO(**a**), (Na_2O + CaO) vs K_2O(**b**), Rb vs K_2O(**c**) and Sr vs CaO(**d**) for typical western quartzofeldspathic gneiss (▲) and types 1 (■) and 2 (•) of the eastern quartzofeldspathic gneiss.

All groups of gneisses display a wide range of chemical composition with respect to the more abundant trace elements Zr, Y, Sr and Rb. Figs 3**c** and 3**d** demonstrate that Rb

TABLE 4

Plagioclase and K-feldspar analyses

	Plagioclase								
	2908	2926	2913	4162	2931	2851	2928	4127	4196
SiO_2	63.75	62.92	61.55	59.84	64.30	62.59	64.17	59.26	61.94
TiO_2									
Al_2O_3	23.34	23.92	24.36	24.18	22.73	23.81	22.57	26.33	24.02
FeO (total iron)									
MnO									
MgO									
CaO	4.08	5.12	5.64	5.82	2.31	4.85	3.29	7.71	5.33
Na_2O	9.06	8.82	8.31	7.64	9.98	9.17	10.15	6.93	8.17
K_2O	.26	.27	.30	.30	.18	.23	.25	.17	.22
TOTALS	100.49	101.05	100.16	97.78	99.50	100.65	100.43	100.40	99.68
	Number of ions on the basis of 32 O								
Si	11.20	11.04	10.91	10.86	11.36	11.03	11.30	10.53	11.00
Al^{iv}	.80	.96	1.09	1.14	.64	.97	.70	1.47	1.00
Al^{vi}	4.04	3.99	4.01	4.04	4.10	3.98	3.98	4.04	4.03
Ca	.77	.96	1.07	1.13	.44	.92	.62	1.47	1.01
Na	3.09	3.00	2.86	2.69	3.42	3.13	3.46	2.39	2.81
K	.06	.06	.07	.07	.04	.05	.06	.04	.05
	Mol %								
Or	1.49	1.50	1.70	1.79	1.04	1.26	1.36	.99	1.29
Ab	78.88	74.58	71.49	69.12	87.74	76.41	83.66	61.31	72.56
An	19.63	23.92	26.81	29.10	11.22	22.33	14.99	37.70	26.16

	K – feldspar								
	2908	2926	2913	4162	2931	2851	2928	4127	4196
SiO_2	65.19	64.83	64.84	63.82	63.25	64.28	63.81	63.93	64.76
TiO_2									
Al_2O_3	19.21	18.47	18.74	18.61	18.77	18.91	19.11	19.42	18.77
FeO (total iron)									
MnO									
MgO									
CaO	.04		.08		.12	.08	.18	.22	.25
Na_2O	1.90	1.14	1.67	1.69	1.51	1.25	2.04	1.96	2.09
K_2O	14.63	15.42	14.44	14.18	15.77	15.49	14.22	14.20	13.73
TOTALS	100.97	99.86	99.77	98.30	99.42	100.02	99.36	99.73	99.60
Si	11.88	11.97	11.94	11.93	11.81	11.88	11.83	11.79	11.93
Al^{iv}	.12	.03	.06	.07	.19	.12	.17	.21	.07
Al^{vi}	4.01	4.00	4.01	4.03	3.96	4.00	4.00	4.02	4.00
Ca	.01		.02		.02	.02	.04	.04	.05
Na	.67	.41	.60	.61	.55	.45	.73	.70	.75
K	3.40	3.63	3.39	3.38	3.76	3.65	3.36	3.34	3.23
Or	83.36	89.90	84.72	84.67	86.81	88.73	81.39	81.78	80.22
Ab	16.45	10.10	14.89	15.34	12.63	10.88	17.75	17.16	18.56
An	.19		.39		.56	.39	.87	1.06	1.23

Analysts: E.R. Phillips and B.E. Chenhall.

and Sr contents are linearly related to K_2O and CaO compositions with 67% and 46% of the variation in Rb and Sr being accounted for by variation in K_2O and CaO respectively. Plots of K_2O/Sr, CaO/Rb and Na_2O/Rb are also essentially linear but these have negative slopes. Throughout all gneisses increase in Zr composition is generally accompanied by an increase in Y.

Phase Data

Chemical data for plagioclase and K-feldspar are presented in Table 4. Generally, there is good agreement between the compositions of plagioclase determined by optical

TABLE 5

Almandine and biotite analyses

	Almandine															
	4150[1]	4150[2]	4150[3]	4151[1]	4151[2]	4151[3]	4152[1]	4152[2]	4162[1]	4162[2]	4162[3]	4128[1]	4128[2]	4128[3]	4196[1]	4196[2]
SiO_2	37.19	37.12	37.48	37.41	36.94	37.49	37.23	37.61	36.68	36.64	36.64	36.99	37.35	37.31	36.55	36.60
TiO_2																
Al_2O_3	21.35	21.39	21.50	20.66	20.65	20.90	21.30	21.68	21.09	20.99	21.15	20.80	21.05	20.87	20.91	21.04
FeO (total iron)	37.41	36.94	38.00	37.87	38.07	38.71	35.98	35.77	38.70	38.37	38.82	35.97	35.41	36.68	38.38	37.46
MnO	1.20	1.07	1.11	.61	.80	.83	.67	.69	.85	.68	.63	1.89	1.37	2.13	1.34	1.41
MgO	3.16	3.54	2.75	2.11	2.28	2.01	4.09	4.72	2.64	2.85	2.48	2.12	3.31	2.09	2.07	2.74
CaO	1.00	.86	.93	.84	.81	.82	.98	.88	.95	.89	.99	2.08	1.89	1.64	1.26	1.33
Na_2O																
K_2O																
TOTALS	101.31	100.92	101.77	99.50	99.55	100.76	100.25	101.35	100.91	100.42	100.71	99.85	100.38	100.72	100.51	100.58
	Number of ions on the basis of 12 0															
Si	2.97	2.97	2.98	3.04	3.01	3.02	2.98	2.97	2.96	2.97	2.96	3.00	2.99	3.00	2.97	2.96
Al^{iv}	.03	.03	.02				.02	.03	.04	.03	.04		.01		.03	.04
Al^{vi}	1.98	1.98	2.00	1.98	1.98	1.99	1.99	1.99	1.97	1.97	1.97	1.99	1.98	1.98	1.97	1.96
Ti																
Fe^{2+}	2.50	2.47	2.53	2.58	2.60	2.61	2 41	2.36	2.61	2.60	2.62	2.44	2.37	2.47	2.61	2.53
Mn	.08	.07	.07	.04	.06	.06	.05	.05	.06	.05	.04	.13	.09	.15	.09	.10
Mg	.38	.42	.33	26	.28	.24	.49	.56	.32	.34	.30	.26	.40	.25	.25	.33
Ca	.09	.07	.08	.07	.07	.07	.08	.07	.08	.08	.09	.18	.16	.14	.11	.12
Na																
K																

	Biotite									
	4150[4]	4150[5]	4151[4]	4151[5]	4152[4]	4162[4]	4162[5]	4128[4]	4128[5]	4196[4]	4196[5]
SiO_2	35.34	36.65	35.41	36.38	35.59	35.51	35.00	35.53	35.42	35.24	34.74
TiO_2	2.71	1.87	2.90	2.59	3.36	3.12	2.19	2.38	1.54	3.05	2.08
Al_2O_3	17.30	18.50	17.46	18.77	17.36	18.35	18.86	17.71	18.07	17 87	17.82
FeO (total iron)	20.52	17.43	20.78	19.55	19.97	21.04	20.06	21.88	21.66	23 57	23.41
MnO											
MgO	8.56	11.13	8.43	8.68	9.08	8.50	9.15	8.09	9.10	6.30	7.06
CaO											
Na_2O	.23	.36				.30	.35			.48	.47
K_2O	9.38	9.88	9.70	9.54	9.51	9.68	9.63	9.54	9.35	9.49	8.82
TOTALS	94.04	95.82	94 68	95.51	95.69	96.50	95.24	95.13	95.14	96.00	94.40
	Number of ions on the basis of 220										
Si	5.50	5.50	5.48	5.51	5.43	5.39	5.36	5.49	5.46	5.45	5.45
Al^{iv}	2.50	2.50	2.52	2.49	2.57	2.61	2.64	2.51	2.54	2.55	2.55
Al^{vi}	.67	.77	66	.86	.64	.67	.77	.72	.74	.71	.74
Ti	.32	.21	.34	.30	.39	.36	.25	.28	.18	.35	.25
Fe^{2+}	2 67	2.19	2.69	2 48	2.55	2 67	2.57	2.83	2.79	3.05	3.07
Mn											
Mg	1.98	2.49	1.94	1.96	2.06	1.92	2.09	1.86	2.09	1.45	1.65
Ca											
Na	.07	.10				.09				.14	.14
K	1.86	1.89	1.91	1.84	1.91	1.88	1.88	1.88	1.84	1.87	1.76

Analyst. B.E. Chenhall

1 rim domain, 2 core domain, 3 garnet composition adjacent to secondary biotite, 4 coarse matrix biotite, 5 secondary biotite adjacent to garnet (3) or garnet rim (1).

and electron microprobe techniques. Moreover, the plagioclase is optically and chemically homogeneous. Bulk microperthite compositions appearing in Table 4 have been obtained by averaging microprobe spot analyses, although some integrated compositions were determined using a defocused (40 μm) electron beam. This technique gave reproducible results on K-feldspars containing fine albite lamellae. The bulk perthite sodium contents are typically less than 2.5% (wt) Na_2O. Sodium contents have generally been found to be lower in the rim domains and higher in the central domains of the larger microperthite crystals.

Table 5 lists compositional data for coexisting garnet and biotite. Garnet compositions were obtained by averaging electron microprobe spot analyses of rim and core areas and domains adjacent to secondary biotite occupying fractures in garnet. All the analysed garnets are iron almandines containing significant molecular pyrope with lesser amounts of spessartine and grossular component. Table 5 shows that MgO/FeO in the rims of garnets is lower relative to their cores and that MgO/FeO is even lower in garnet adjacent to secondary biotite. Electron microprobe rim-rim traverses across four garnet grains are presented in Fig. 4. These profiles demonstrate that a strong inverse relationship exists between the Mg and Fe contents measured across the grains, whereas Ca and Mn are relatively evenly distributed throughout these almandines.

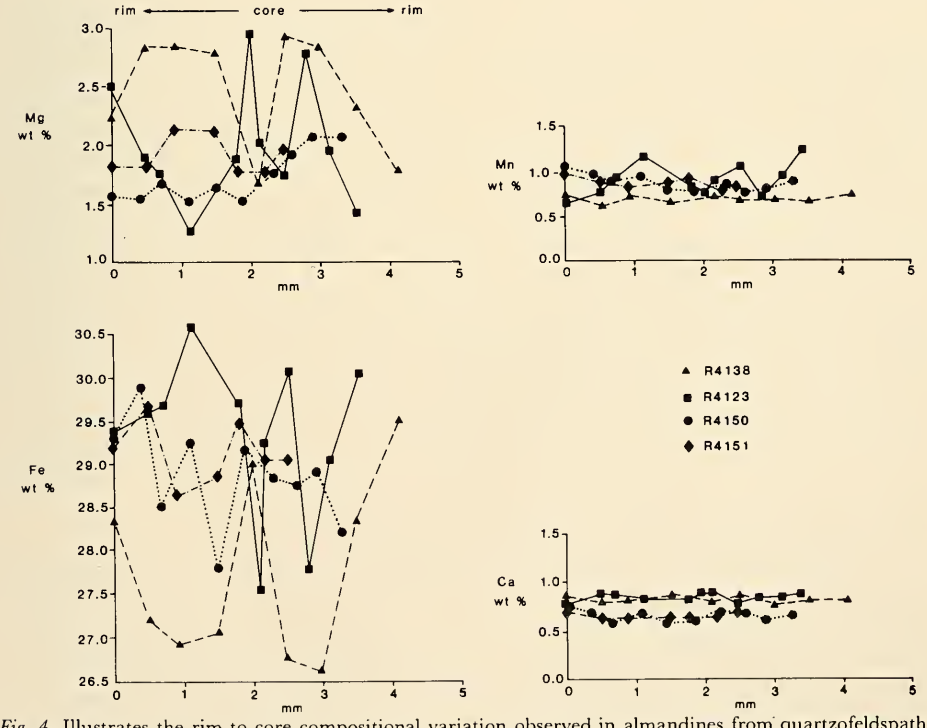

Fig. 4. Illustrates the rim to core compositional variation observed in almandines from quartzofeldspathic gneisses. Specimen numbers refer to rocks housed in the Department of Geology, University of Wollongong.

Electron microprobe traverses across coarse biotite forming the foliation in these gneisses show that these grains are homogeneous with respect to their FeO, MgO and TiO_2 compositions. Coarse biotites have lower MgO/FeO and higher TiO_2 compared with the finer secondary fracture-filling biotites.

Discussion

The most characteristic microstructural association common to K-feldspar-bearing samples of both the western and eastern quartzofeldspathic gneisses is one in which various morphological forms of microperthite are consistently observed in close spatial arrangement with domains containing myrmekite, myrmekite plus albite or albite alone. Some idea of the diverse relationships displayed by minerals in this association is afforded by rocks within type 1 of the eastern gneiss where two distinctive microstructural subtypes can be recognized. In the first of these, coarse bead and fine film perthite (containing a considerable amount of plagioclase) are associated with myrmekite-free areas containing rim and intergranular albite; whereas in the second subtype, sparse film perthites are developed with either rim myrmekite (An_{15}-An_{17}) and albite or with intergranular myrmekite and albite (see also Phillips and Stone, 1974). Petrographic observations indicate that the bead perthites have higher Na_2O contents compared with the sparse film perthites and, together with the microstructural differences noted above and range in the structural state of the K-feldspar from orthoclase to intermediate microcline, lend credence to the contention that these gneisses have undergone a relatively complex metamorphic history.

Perthites are usually thought to represent the products of exsolution during cooling (Smith, 1974) with the regularity and preferred orientation of the sodic plagioclase lamellae providing strong evidence in support of this interpretation (Yund and Ackermand, 1979). Phillips, Ransom and Vernon (1972) have proposed that myrmekite in quartzofeldspathic ('Potosi') gneiss from the mine sequence (Suite 4) has a polygenetic origin, most being produced by an exsolution mechanism whereas minor amounts of myrmekite originated from retrograde decomposition of K-feldspar with the concomitant production of muscovite. An exsolution process may also account for the development of rim and intergranular myrmekite and albite throughout most of the eastern and western quartzofeldspathic gneisses. A retrograde reaction model cannot adequately explain the observed microstructural relationships between the felsic phases, since muscovite is absent from or is present only in small amounts in these gneisses and furthermore, muscovite where present has no consistent microstructural association with either myrmekite or albite. Sodium-depleted rim domains in K-feldspar are possibly produced by exsolving sodium in the form of myrmekite and rim albite. Alternative diffusion or reaction mechanisms involving loss of sodium to the matrix plagioclase (Bohlen and Essene, 1977) do not offer a satisfactory explanation for the sodium-depleted domains in K-feldspar. These models cannot account for the essentially homogeneous nature of plagioclase throughout all domains in the rocks nor can they explain the presence of intergranular myrmekite and albite in plagioclase-free domains between adjacent K-feldspars.

Grainsize coarsening of microperthite lamellae due to reduction of interfacial free energy between phases in the intergrowths (Yund and Ackermand, 1979) and variation in the original bulk perthite composition are other factors which may control the morphology of microperthites in quartzofeldspathic gneisses at Broken Hill. Intergranular/intragranular diffusion rates are probably accelerated in the presence of an aqueous phase (Yund and Ackermand, 1979; Parsons, 1978) leading to the development of coarse, incoherent microperthite intergrowths. However, we cannot convincingly demonstrate that the diverse microperthites described above originate due to variations in the

concentration or activity of a fluid phase because the host gneisses appear to have largely cooled under conditions where either the concentration or activity of volatiles or P_{H2O} was low. Variation in bulk microperthite composition is presumably related to differences in 'peak' metamorphic temperature but the bulk K-feldspar compositions appearing in Table 4 do not preserve a true record of the thermal history of the quartzofeldspathic gneisses. 'Peak' metamorphic temperatures may be estimated using a plagioclase—K-feldspar geothermometer (Stormer, 1975) assuming initial equilibrium between coexisting feldspars and provided that the microperthite analyses are integrated to give original bulk K-feldspar compositions (Bohlen and Essene, 1977). This procedure cannot be successfully applied to the gneisses in this study. Coexisting microperthite-plagioclase compositions yield unrealistically low (usually $<600°C$) estimates of 'peak' metamorphic temperature primarily because at least part of the sodic component is lost in the form of myrmekite and albite. Furthermore, little significance can be attached to the derived temperature estimates since the intergranular microstructures probably represent disequilibrium between the felsic phases of the rocks.

Orthoclase is the common K-feldspar phase throughout the bulk of the western and eastern quartzofeldspathic gneisses and its persistence in these rocks could well be related to their cooling histories (see also Guidotti, Herd and Tuttle, 1973). However, it is generally assumed that the very slow cooling rates which accompany regional metamorphism should serve to promote increased Al/Si ordering of K-feldspar leading to the production of microcline, provided of course that diffusion rates are sufficiently high over the cooling interval where microcline is stable. Parsons (1978) has clearly demonstrated that increased ordering in K-feldspar can be related to higher local activities or concentrations of volatile phases. These could provide some samples with faster rates of diffusion resulting in the development of more ordered feldspar lattices.

The persistence of orthoclase thus may be attributable to low activities or concentrations of water and consequently imply 'dry' cooling histories for the gneisses at Broken Hill. Such a proposal is supported by the water activity data obtained by Phillips (1980) for metapelites (a_{H_2O} = 0.5-0.6) in the Broken Hill mines area. One further comment seems warranted here. Wright (1967) has estimated the upper stability limit of maximum microcline to be 375 ± 50°C. Elsewhere in this study it is suggested that temperatures controlling the effective Mg/Fe exchange between almandine and fine grained (secondary) biotite lie above this estimate (at $>$ 450°C). Thus it may be tentatively suggested that orthoclase could persist in 'dry' rocks if very low diffusion rates prevailed during the final stages of cooling. Intermediate microcline locally present in the eastern gneiss, could evolve due to an increase in volatile activity or concentration associated with prograde metamorphism, but this notion is not supported by the relatively constant nature of water activity estimates for any given locality in the Broken Hill district (Phillips, 1980). Alternatively, increased ordering of the K-feldspar lattice could be promoted by the onset of retrogression where water activities or P_{H_2O} were probably much higher (Chenhall, 1973).

Thus our findings regarding the evolution of these microstructures remain essentially qualitative. However, we do believe that different degrees of exsolution during cooling (under conditions where a low concentration or activity of a volatile phase prevailed) can offer a plausible explanation for the development of these microstructures and the disordered nature of the K-feldspar in the gneisses. Further, we suggest that later retrograde metamorphism could serve to modify further the microstructures that we have described.

Although there is chemical evidence for the homogenization of matrix biotite and almandine compositions (for example the central portion of profile R 4138, Fig. 4) during prograde metamorphism, the microstructures of coexisting biotite and garnet, together

with the observed compositional differences of biotite-garnet domains (Table 5 and Fig. 4) are highly suggestive of a retrograde reaction relationship involving the partial decomposition of almandine to form biotite. Compositional heterogeneity in garnet can generally be interpreted in terms of growth fractionation, diffusion exchange or diffusion reaction models (Loomis, 1975). Several authors (e.g. Evans and Guidotti, 1966; Hollister, 1969) have demonstrated that the compositional variation preserved in garnet can suggest reactions which took place between these garnets and the matrix phases of the rock. For example, Hollister (1969) attributed increase in Ti and Mn in the rims of garnet to the decomposition of matrix ilmenite. Elemental distribution profiles (Fig. 4) and Table 5 show that Ca and Mn are fairly evenly distributed throughout garnet with Ti values (Table 5) below the limits of detection of the microprobe. Thus it may be reasonably concluded on the basis of this and on textural grounds that the matrix phases, ilmenite and plagioclase, containing these components have not reacted to produce either garnet or biotite. The asymmetric nature of and the pronounced 'sawtooth' configuration of the Mg-Fe profiles are related to the spatial arrangement of garnet and biotite, higher Mg/Fe in almandine characterizing those domains in which biotite is not in contact with or found immediately adjacent to garnet (see also Tracy, Robinson and Thompson, 1976: 767-768). These observations suggest that the relationship between the two ferromagnesian phases may be best modelled according to a diffusion exchange reaction of the form:

$$Mg_3Al_2(SiO_4)_3 + KFe_3AlSi_3O_{10}(OH)_2 = Fe_3Al_2(SiO_4)_3 + KMg_3AlSi_3O_{10}(OH)_2 \quad . . .(1)$$

Mg in garnet + Fe in biotite = Fe in garnet + Mg in biotite

However, it is apparent from petrographic observations and from the Ti contents of biotites that the model is probably more complex and also involves the production of a low Ti biotite together with small volumes of a Ti-rich phase (ilmenite). Reactions of this type are currently being investigated by one of us (BEC).

Compositions of coexisting almandine and biotite offer a potentially useful means of estimating temperatures of formation of metamorphic rocks provided either that the garnets are homogeneous or that their heterogeneous nature can be fully taken into account. For chemically-zoned garnets, substantial errors in temperature estimates arise where significant compositional shifts in Mg/Fe of biotite have taken place during garnet growth (Tracy, Robinson and Thompson, 1976: 768). Noting the compositional complexity displayed by garnets in this study, it appears most unwise to calculate temperatures following the compositional models proposed by these workers. Instead, we have calculated temperatures at 5kb pressure (based on equation 7 of Ferry and Spear, 1978) from the Mg/Fe values of biotite and garnet grain contacts assuming that these phases are in local equilibrium. These yield values in the range 450-580°C. Clearly these estimates give no indication of 'peak' prograde metamorphic temperatures but they seem useful in that they assist in placing constraints on the temperature interval over which interdiffusion was effective in distributing Fe and Mg between biotite and garnet.

Compositional data for Fe-Mg biotite and almandine in metapelitic gneisses, and in particular, the compositional shift of these phases towards more Mg-rich end members (Phillips, 1980) provide direct evidence for an increase in prograde metamorphic temperatures from northwest to southeast across the Broken Hill Block. This grade increase is also reflected in rocks containing biotite and garnet occurring immediately to the northwest and southeast of the Broken Hill orebody (Plimer, 1976).

In the western and eastern quartzofeldspathic gneisses, compositional shifts of the ferromagnesian phases towards more Mg-rich end members in response to increasing temperature, are generally overprinted by the retrograde compositional adjustments noted above. However, the data of Fig. 4 (profiles R 4123 and 4138) suggest that at least

garnet Mg contents tend to be higher in type 2 eastern quartzofeldspathic gneisses occurring to the east and southsoutheast of the orebody.

Furthermore, our studies and those of previous workers (Stone, 1973; Pemberton, 1977) have drawn attention to the widespread occurrence of generally small (0-4%) modal amounts of sillimanite in rocks from the western quartzofeldspathic gneiss and to the virtual absence of this phase in rocks of the eastern mass. The distribution pattern of sillimanite in these quartzofeldspathic rocks is somewhat elusive. However, differences in bulk rock composition, for example in molar $Al_2O_3/(K_2O + Na_2O + CaO)$ cannot completely account for this pattern since rocks with similar chemistry are represented in both rock suites. A possible explanation for the absence of sillimanite in samples of the eastern gneiss is that during prograde metamorphism this phase (or equivalent component) was consumed according to a reaction of the form:

$$\underset{\text{biotite}}{K(MgFe)_3AlSi_3O_{10}(OH)_2} + \underset{+\ \text{sillimanite}}{Al_2SiO_5} + \underset{+\ 2\ \text{quartz}}{2SiO_2} =$$

$$\underset{\text{almandine}}{(MgFe)_3Al_2(SiO_4)_3} + \underset{+\ \text{K-feldspar}}{KAlSi_3O_8} + \underset{+\ \text{water}}{H_2O} \qquad \ldots (2)$$

which represents bivariant equilibrium for fixed activity of water at any given pressure.

Thus the compositional data for coexisting ferromagnesian phases and the absence of sillimanite in the eastern quartzofeldspathic gneiss appear to be compatible with sliding of bivariant reactions (equation 2) to their higher entropy side at elevated temperatures.

The pre-metamorphic nature of the quartzofeldspathic gneisses at Broken Hill is subject to some conjecture. Previously, workers have suggested that some or all of these rocks may represent metamorphosed igneous rocks (Binns, 1964) or metamorphosed sediments (Stillwell, 1922). However, it is clear that within the gneisses described above, original microstructures which could possibly unambiguously resolve the nature of their parent material are not preserved due to complete recrystallization at high metamorphic temperatures. Preliminary work by Wall, Etheridge and Hobbs (1976), Stevens *et al.* (1980) and the unpublished work of Shaw together tend to indicate a general chemical link between the quartzofeldspathic gneisses and volcanic (or igneous) precursors. Thus it seems appropriate in this study to compare the chemical compositions of the analysed gneisses with those of commonly-occurring igneous and sedimentary rocks and to suggest likely parent materials for them on this basis.

Apart from several examples, the compositional data for the major variety of the western quartzofeldspathic gneiss (Table 2) and type 2 of the eastern gneiss (Table 3) appear to be consistent with their derivation from pre-existing igneous rocks chemically akin to rhyodacite or dacite. The average major element composition of these gneisses is close to Nockolds' (1954) average rhyodacite or plutonic equivalent. Exceptions to this generalization are manifested in the lower mean CaO, Na_2O and slightly higher total iron (FeO) values of both gneisses and also by the higher average SiO_2 value for the major type of western quartzofeldspathic gneiss. Type 1 eastern gneiss samples (Table 3) are chemically distinct from the other gneisses and are similar in composition to rhyolites or their intrusive equivalents, with the average composition of this gneissic type closely matching Nockolds' (1954) average rhyolite composition.

Chemical variation diagrams (Figs 2 and 3) indicate that there is generally linear compositional variation between selected major oxides and major oxides-trace elements throughout the three major varieties of quartzofeldspathic gneiss. Some interoxide plots, notably Al_2O_3/FeO and $K_2O/(Na_2O + CaO)$, show much more scatter. Chayes (1971) has fully described and discussed the statistical limitations inherent to geochemical interpretation of variation diagrams where the data consist of ratios or percentages. These limitations notwithstanding, we believe that the linear variation displayed by various

combinations of oxides and trace elements is better explained in terms of a pre-metamorphic igneous source material rather than by materials having composite or mixed (volcano-sedimentary) parentage. Variation in some oxides notably alkalis and calcium may reflect the original variability of parent material compositions or may be related to pre-metamorphic alteration (Wall, Etheridge and Hobbs, 1976) or to transfer of chemical components during retrogression. The last suggestion is not favoured since lower temperature microstructural and chemical adjustments appear to have taken place on the intergranular or intragranular scale and thus there seems little reason to account for the variation in this manner. It appears unlikely that the quartzofeldspathic gneisses could have undergone extensive pre-metamorphic alteration because this process could reasonably be expected to result in more complex interelemental distributions throughout them.

Representative samples of 'amphibolite/basic granulite' interlayered with the quartzofeldspathic rocks have been interpreted as the metamorphosed derivatives of highly fractionated tholeiitic rocks (Plimer, 1975; Stevens, 1978). Indeed, Stevens *et al.* (1980) suggest that the close spatial association and chemical characteristics of these contrasted rock types are consistent with several pre-metamorphic pulses of paired acid-basic vulcanism. Other rock types occurring throughout the western and eastern quartzofeldspathic gneiss have compositions (e.g., Table 3: analyses 4142, 4127, 4199) which are considered to be atypical of igneous parent material. We tentatively suggest that these rocks represent metamorphosed examples of quartzofeldspathic sediments.

Thus our data suggest a link between the three main types of quartzofeldspathic gneiss that we have studied and acid igneous precursors. Furthermore, the lithological, mineralogical and chemical diversity observed by us and by other workers throughout the western and eastern quartzofeldspathic gneiss seems consistent with the interpretation that both of these bodies represent a composite pile of metamorphosed volcanic rocks and interlayered sediments.

Acknowledgements

Our thanks are extended to David Klingner, Ian Johnson and Bill Widdop for providing diamond drill core logs and their assistance with selection of samples. Drs S. E. Shaw and R. H. Flood provided major element analyses of most rocks. Preparation of the manuscript would not have been possible without the use of the electron microprobe facilities of the British Museum (Natural History) and Department of Earth Sciences, University of Cambridge and of the XRF facility, Department of Geology, University of Wollongong. David Martin drafted the figures and Margaret Atkinson and Jenny Jarman typed the manuscript. We are grateful to Prof. T. G. Vallance and Dr B. G. Jones for their constructive comments regarding preparation of the paper. The tenure of a University of Wollongong research grant is especially acknowledged.

References

Andrews, E. C., 1922. — The geology of the Broken Hill district. *Mem. Geol. Surv. N.S.W.* 8.

Binns, R. A., 1962. — Studies in metamorphism at Broken Hill, New South Wales. Cambridge: University of Cambridge PhD thesis, unpubl.

——, 1964. — Zones of progressive regional metamorphism in the Willyama Complex, Broken Hill District, New South Wales. *J. geol. Soc. Aust.* 11: 283-330.

Bohlen, S. R., and Essene, E. J., 1977. — Feldspar and oxide thermometry of granulites in the Adirondack Highlands. *Contrib. Mineral. Petrol.* 62: 153-169.

Carruthers, D. S., and Pratten, R. D., 1961. — The stratigraphic succession and structure in the Zinc Corporation Ltd and New Broken Hill Consolidated Ltd, Broken Hill, New South Wales. *Econ. Geol.* 56: 1088-1102.

Chayes, F., 1971. — *Ratio Correlation.* Chicago: University of Chicago Press.

Chenhall, B. E., 1973. — Some aspects of prograde and retrograde metamorphism at Broken Hill. Sydney: University of Sydney PhD thesis, unpubl.

——, 1976. — Chemical variation of almandine and biotite with progressive regional metamorphism of the Willyama Complex, Broken Hill, New South Wales. *J. geol. Soc. Aust.* 23: 235-242.

——, PHILLIPS, E. R., STONE, I. J., and PEMBERTON, J. W., 1977. — Gneisses at Broken Hill, N.S.W. *Mineral. Mag.* 41: M20.

EVANS, B. W., and GUIDOTTI, C. V., 1966. — The sillimanite-potash feldspar isograd in Western Maine, U.S.A. *Contrib. Mineral. Petrol.* 12: 25-62.

FERRY, J. M., and SPEAR, F. S., 1978. — Experimental calibration of the partitioning of Fe and Mg between biotite and garnet. *Contrib. Mineral. Petrol.* 66: 113-117.

GUIDOTTI, C. V., HERD, H. H., and TUTTLE, C. L., 1973. — Compositional and structural state of K-feldspars from K-feldspar + sillimanite grade rocks in Northwestern Maine. *Amer. Mineral.* 58: 705-716.

HOBBS, B. E., 1966. — The structural environment of the northern part of the Broken Hill orebody. *J. geol. Soc. Aust.* 13: 315-338.

HOLLISTER, L. S., 1969. — Contact metamorphism in the Kwoiek area of British Columbia. An end member of the metamorphic process. *Bull. Geol. Soc. Amer.* 80: 2465-2494.

JOHNSON, I. R., and KLINGNER, G. D., 1975. — The Broken Hill ore deposit and its environment, *in* Economic Geology of Australia and Papua New Guinea. 1. Metals. *Australas. Inst. Min. Metall., Monogr.* 5: 476-491.

KING, H. F., and O'DRISCOLL, E. S., 1953. — The Broken Hill lode. *In* Geology of Australian Ore Deposits. *Empire Mining and Metallurgical Congress, 5th, Australia and New Zealand. Publ.* 1: 578-600.

LAING, W. P., MARJORIBANKS, R. W., and RUTLAND, R. W. R., 1978. — Structure of the Broken Hill mine area and its significance for the genesis of orebodies. *Econ. Geol.* 73: 1112-1136.

——, 1980. — Stratigraphic interpretation of the Broken Hill mines area. *In* STEVENS, B. P. J., (ed.), A guide to the stratigraphy and mineralization of the Broken Hill Block, New South Wales. *Rec. Geol. Surv. N.S.W.* 20(1): 71-85.

LOOMIS, T. P., 1975. — Reaction zoning of garnet. *Contrib. Mineral. Petrol.* 52: 285-305.

MAWSON, D., and SEGNIT, E. R., 1946. — Barium-rich aplitic gneisses at Broken Hill. *Trans. R. Soc. S. Aust.* 70: 277-293.

NOCKOLDS, S. R., 1954. — Average chemical compositions of some igneous rocks. *Bull. Geol. Soc. Amer.* 65: 1007-1032.

PARSONS, I., 1978. — Feldspars and fluids in cooling plutons. *Mineral. Mag.* 42: 1-17.

PEMBERTON, J. W., 1977. — A further study of the quartzofeldspathic gneisses associated with the Broken Hill orebody, Broken Hill, New South Wales. Wollongong: University of Wollongong BSc (Hons) thesis, unpubl.

PHILLIPS, E. R., RANSOM, D. M., and VERNON, R. H., 1972. — Myrmekite and muscovite developed by retrograde metamorphism at Broken Hill, New South Wales. *Mineral. Mag.* 38: 541-544.

——, and STONE, I. J., 1974. — Reverse zoning between myrmekite and albite in a quartzofeldspathic gneiss from Broken Hill, New South Wales. *Mineral. Mag.* 39: 654-657.

PHILLIPS, G. N., 1980. — Water activity changes across an amphibolite-granulite facies transition, Broken Hill, Australia. *Contrib. Mineral. Petrol.* 75: 337-386.

PIDGEON, R. T., 1967. — A rubidium-strontium geochronological study of the Willyama Complex, Broken Hill, Australia. *J. Petrol.* 8: 283-324.

PLIMER, I. R., 1975. — The geochemistry of amphibolite retrogression at Broken Hill, Australia. *Neues. Jahrb. Mineral. Abh.* 10: 471-481.

——, 1976. — Garnet-biotite relationships in high grade metamorphic rocks at Broken Hill, Australia. *Geol. Mag.* 113: 263-270.

SCOTT, S. D., BOTH, R. A., and KISSIN, S. A., 1976. — Sulfide petrology of the Broken Hill region, New South Wales, Australia. In *25th Int. Geol. Congr. Abs.* (1): 140-141.

SHAW, S. E., 1968. — Rb-Sr isotopic studies of the mine sequence rocks. *In* RADMANOVICH, M., and WOODCOCK, J. T., (eds.), Broken Hill Mines. *Aust. Inst. Min. Metall. Monogr.* 3: 185-198.

SMITH, J. V., 1974. — *Feldspar Minerals:* Vol. 2, *Chemical and textural properties.* Berlin, Heidelberg, New York: Springer Verlag.

STEVENS, B. P. J., 1978. — The geological environment of mineralisation in the Centennial-Great Western area, Broken Hill. Sydney: University of Sydney MSc thesis, unpubl.

——, STROUD, W. J., WILLIS, I. L., BRADLEY, G. M., BROWN, R. E., and BARNES, R. G., 1980. — A stratigraphic interpretation of the Broken Hill Block. *In* STEVENS, B. P. J., (ed.), A guide to the stratigraphy and mineralization of the Broken Hill Block, New South Wales. *Rec. Geol. Surv. N.S.W.* 20(1): 9-32.

STILLWELL, F. L., 1922. — The rocks in the immediate neighbourhood of the Broken Hill Lode and their bearing on its origin. *In* ANDREWS, E. C., (ed.), The geology of the Broken Hill district. *Mem. Geol. Surv. N.S.W.* 8: 354-396.

STONE, I. J., 1973. — The quartzofeldspathic gneisses associated with the Broken Hill orebody, Broken Hill, N.S.W. Wollongong: University of Wollongong BSc(Hons) thesis, unpubl.

STORMER, J. C., 1975. — A practical two-feldspar geothermometer. *Amer. Mineral.* 60: 667-674.

TRACY, R. J., ROBINSON, P., and THOMPSON, A. B., 1976. — Garnet composition and zoning in the determination of temperature and pressure of metamorphism, central Massachusetts. *Amer. Mineral.* 61: 762-775.

VERNON, R. H., 1969. — The Willyama Complex, Broken Hill area. *In* PACKHAM, G. H., (ed.), The Geology of New South Wales. *J. geol. Soc. Aust.* 16(1): 20-55.

——, and RANSOM, D. M., 1971. — Retrograde Schists of the amphibolite facies at Broken Hill, New South Wales. *J. geol. Soc. Aust.* 18: 267-277.

WALL, V. J., ETHERIDGE, M. A., and HOBBS, B. E., 1976. — Pre-metamorphic features of Broken Hill lode/host rocks and their bearing on the origin of mineralization. In *25th. Int. Geol. Congr. Abs.* (1): 197-198.

WRIGHT, T. L., 1967. — The microcline-orthoclase transformation in the contact aureole of the Eldora Stock, Colorado. *Amer. Mineral.* 52: 117-136.

YUND, R. A., and ACKERMAND, D., 1979. — Development of perthite microstructures in the Storm King Granite, N.Y. *Contrib. Mineral. Petrol.* 70: 273-280.

APPENDIX

Locality Information for the Representative Samples of Quartzofeldspathic Gneiss

Western Quartzofeldspathic Gneiss

(a) Quartz + plagioclase + K-feldspar + biotite ± almandine ± sillimanite gneisses

number	locality
2908	D.D.H. 3176; 118m below collar
2926	g.r. 1779000E 21203500N
2913	D.D.H. 2550; 203m below collar
4150, 2916	D.D.H. 2870; 435m and 533m below collar respectively
4154	D.D.H. 2460; 589m below collar
4162	D.D.H. 2290; 1042m below collar

(b) Quartz + plagioclase + biotite ± K-feldspar ± almandine ± sillimanite gneisses

number	locality
4409	D.D.H. 3167; 1211m below collar
2903	g.r. 1792000E 21210000N
2835	g.r. 1793000E 21211000N
4171	D.D.H. 2550; 777m below collar
4151	D.D.H. 2870; 625m below collar
4152, 4153	D.D.H. 2460; 411m and 476m below collar respectively
2902	g.r. 1860000E 21178000N
2897	g.r. 1769000E 21175700N
2858	D.D.H. KC5; 322m below collar

Eastern Quartzofeldspathic Gneiss
Type 1 Gneisses

(a) Quartz + plagioclase + K-feldspar + biotite ± almandine gneisses

number	locality
4119	g.r. 1811800E 21223600N
2931	g.r. 1801250E 21209000N
2851	D.D.H. 3113; 188m below collar
2928	g.r. 1804500E 21207000N
4120	g.r. 1811800E 21223600N
4205	g.r. 1810000E 21200000N
4194	g.r. 1777000E 21176000N
4196	g.r. 1765000E 21175000N

(b) Quartz + plagioclase + biotite ± K-feldspar ± almandine gneisses

number	locality
4392, 4396	D.D.H. 3186; 313m and 543m below collar respectively
2932	g.r. 1809000E 21221000N

Type 2 Gneisses

(a) Quartz + plagioclase + K-feldspar + biotite ± almandine gneisses

number	locality
2862	g.r. 1792000E 212050000N

(b) Quartz + plagioclase + biotite ± K-feldspar ± almandine gneisses

number	locality
4123, 4124, 4128, 4129	D.D.H. 2770; 49m, 65m, 148m, and 181m below collar respectively
4189	D.D.H. 1560A; 2478m below collar
4138, 4139	D.D.H. 2630; 142m and 180m below collar respectively
4384	D.D.H. 2660; 712m below collar
4386	D.D.H. 2620; 338m below collar

Quartz and Feldspar-Rich Minor Rock Types in the Eastern Quartzofeldspathic Gneiss

number	locality
4142	D.D.H. 2630; 346m below collar
4127	D.D.H. 2770; 136m below collar
4199	g.r. 1767000E 21178000N

Numbers refer to specimens housed in the Department of Geology, University of Wollongong reference collections. Grid references are given for surface samples; diamond drill hole collar locations are to be found in Figure 1B.